Unraveling the Role of Tumor Extracellular Vesicles in Angiogenesis to Inform the Design of Biomimetic Electronic Devices

A Thesis Submitted in Partial Fulfillment of the Requirements

for the Degree of Master of Science at Cornell University

by

Alexus Daishon Locke

Cornell University

August 2021

Thesis Committee:

Susan Daniel, Ph.D., Advisor

Lara Estroff, Ph.D.

Unraveling the Role of Tumor Extracellular Vesicles in Angiogenesis to Inform the Design of Biomimetic Electronic Devices

Abstract

Extracellular vesicles (EVs) are lipid-bilayer particles secreted by various types of cells, including tumor cells. EVs are enriched with a discrete set of bioactive cargoes they can transfer to cells in both adjacent and distant sites to orchestrate multiple key pathophysiological events such as angiogenesis and cancer progression. Although several studies have emerged to probe and characterize these particles, the mechanisms involved in how EVs mediate their cargo transfers are still poorly understood. Accordingly, the development of model systems that may be able to recapitulate and expound upon these mechanisms have become attractive targets. Individually, supported lipid bilayers (SLBs) and organic electrochemical transistors (OECTs) have emerged as novel methods to study and monitor cellular functions. When combined, they have the potential to represent a versatile electronic biosensor capable of monitoring the properties and behavior of mammalian cell surfaces. Here, this hybrid SLB-OECT system is intended to analyze tumor EV (TEV) processes like binding, fusion, and potentially cargo transfer processes on model cell membranes in real-time. In this work, the interactions between TEVs and epithelial cells were studied to assess their ability to induce angiogenesis. The analyses revealed enhanced proangiogenic activity via Vascular Endothelial Growth Factor (VEGF) upregulation amongst cells infected with TEVs. In an effort to evade the effects of TEV exposure, they were treated with heparin to prevent the binding and uptake of TEVs by recipient epithelial cells. Cells exposed to heparin-coated TEVs showed minimal VEGF upregulation similar to the VEGF expression observed of untreated cells indicating successful TEV blocking. These results represent important feedback anticipated to aid in optimizing the design of the aforementioned model SLB-OECT device for the in-depth, mechanistic analysis of TEV-mediated processes.

BIOGRAPHICAL SKETCH

Alexus Locke, born in Harvey, LA and raised in Cypress, TX, graduated from Lamar University with her bachelor of science degree in Mechanical Engineering with a minor in Mathematics in May of 2019. During her time at Lamar, she served in leadership roles in organizations such as Lions Club International and Tau Beta Pi Engineering Honors Society. She also received several awards and honors including being named a Senior of Significance for Lamar's 2019 graduating class.

In research, Alexus was selected to become a McNair Scholar and conduct an independent research study on cancer cell stiffness as a part of the 2016-2017 McNair Scholar's Program cohort. In the summer of 2018, Alexus was chosen to participate in the Research Experience for Undergraduates (REU) program at Johns Hopkins University's Institute for Nanobiotechnology, where she conducted research alongside graduate students in the lab of Dr. Denis Wirtz. Alexus was also awarded two consecutive undergraduate research grants by Lamar University to conduct studies under the joint guidance of Dr. Ping He and Dr. Ian Lian of the Mechanical Engineering and Biology departments, respectively.

Following her graduation from Lamar, Alexus moved to Ithaca, NY, where she conducted research under the guidance of Dr. Susan Daniel of the Robert Frederick Smith School of Chemical and Biomolecular Engineering. There, she worked to investigate the dynamic interactions of cancer extracellular vesicles and epithelial cells. Alexus will graduate with her master of science degree in Chemical Engineering with a concentration in Biochemical Engineering in August of 2021.

ACKNOWLEDGMENTS

It is with profound pleasure, humility, and sincerity that I thank those whose help and support have made the completion of this milestone possible.

First and foremost, I would like to thank my parents who have been a constant source of love and support. Their lives and sacrifices have always been a source of inspiration, teaching me the values of hard work, compassion, and always pursuing my dreams. Thank you to my best friend Victoria, as well, who is an integral part of my support system constantly pushing me to see beyond what is in front of me and fight for the best current and future versions of myself.

The utmost and sincerest thank you to Dr. Susan Daniel for her mentorship, patience, and support. She has been an inspiring mentor and has given me the opportunity to explore my interests. I am so grateful that she welcomed me to join her lab and nurtured my passion for research. With her guidance, I have learned a great deal about work ethic and dedication to science.

Thank you to the members of the Daniel Lab, who have been a fantastic group of people to work with and glean wisdom from over the last two years.

Lastly, I would like to thank Dr. Lara Estroff for agreeing to be on my committee and witness the conclusion of my Master's degree.

TABLE OF CONTENTS

Chapter 1: Introduction

1.1. General Introduction

Metastasis, the spread of cancer cells to a secondary site, remains the leading cause of death for cancer patients worldwide[1,2]. Despite the progress that has been made in cancer research to date, there is still much to be learned about the mechanisms that promote metastasis. Therefore, for future cancer therapies to be successful and efficacious, detailed knowledge of these mechanisms is necessary. Emerging evidence suggests that metastasis is not a cancer cell-autonomous function, rather a collective effort that requires the support of the surrounding tumor tissue[3,4]. This complex environment consists of multiple components, including stromal cells, the extracellular matrix (ECM), surrounding blood vessels, and signaling molecules, which are collectively known as the tumor microenvironment (TME)[3,5]. While a healthy TME is known for its tumor antagonizing behavior[6], rigorous scientific studies have identified the ability of cancer cells to communicate with and modulate components within the TME to generate an environment that is tolerant for tumor growth and spread[7–10].

One target of study that has emerged recently is extracellular vesicles (EVs). EVs are lipid-bilayer particles secreted by several types of eukaryotic cells. There are two major subpopulations of EVs based on their biogenesis (Fig. 1): exosomes (30–150 nm in diameter), which are generated from late endosomes and multivesicular bodies, and microvesicles (0.1–1 μm), which bud directly from the plasma membrane[11,12]. Both types of EVs have been found to display adhesion molecules on their surface[13] and encapsulate various types of cargoes including proteins, lipids, DNA, mRNAs, and miRNAs[14,15]. Extensive research has shown that EVs are an important avenue for intracellular communication through what seems to be orchestrated and deliberate processes of transferring their molecular contents via uptake and release into recipient cells[16]. Through tumor-

derived EVs (TEVs), cancers have found a way to commandeer both malignant and non-malignant cells in the TME to facilitate tumorigenesis by regulating tumor angiogenesis, immunity, and metastasis [11,14,15,17–19].

Despite the rapid rise in research interests seeking to explore these particles and their contents for potential uses as novel cancer diagnostic tools, the ability to accurately model and analyze EV transfer between cells remains a major challenge. To visualize this transfer *in vivo*, studies have employed methods to genetically modify cells which will then release TEVs containing labeled components for tracking through intravital microscopy on the animals involved[20–23]. While transfer was successfully observed in these cases, the mechanisms involved in TEV transfer or the contents of the TEVs involved in the transfers were still not clear. Thus, not only is there a need for tools to study the interactions between TEVs and recipient cells but also, to simultaneously identify the composition of EVs.

Supported lipid bilayers (SLBs), may represent an ideal method to study the interactions between membranes TEVs and stromal cells as they have been widely employed to study and monitor interactions between biomolecules and cell membranes[11,24–27]. Due to their two-dimensional lateral fluidity, tunable nature, and physical stability, SLBs can provide proper orientation and mobility of incorporated biological components, such as lipids and proteins, and are compatible with many surface characterization tools and optical microscopy. Despite these advantages, sizeable barriers remain when attempting to model the native membrane, namely maintaining fluidity, orientation, and function of native lipids and proteins[28]. The most significant hurdle is the purification and incorporation of these native components. In previous work, the Daniel Group has found a way around this hurdle and advanced this system by developing methods to incorporate native plasma cell membrane material through cell blebs that preserve the original

orientation and function of the membrane proteins from mammalian[29], bacterial[30], and most recently TEV membranes[24]. This coupled with another novel assay developed in the Daniel lab which integrates SLBs and single-particle tracking (SPT) represents a promising platform for examining the binding and fusion between TEVs and cells in a unique way.

Another widely used tool for real-time cell monitoring is electrical devices, like organic electrochemical transistors (OECTs). OECTs are polymer-based conducting devices that have been shown to outperform many biosensors due to their high transconductance, biocompatibility, ionic-electronic conductivity, and versatility[31,32]. The integration of OECTs with live cells has most notably been used to sense changes in paracellular ion flux which can indicate changes in cell morphology and integrity[33]. To address the need for simultaneous compositional and functional analysis, the Daniel lab and collaborators have recently been combined SLB technology with OECT technology to provide a novel approach to mimicking and monitoring the properties of mammalian cell surfaces[34–37]. Here, we aim to extend this to cancer studies to analyze the TEV binding, fusion, and potentially cargo transfer processes in real-time.

Ultimately, this thesis contributes to the goal of developing a sensitive analytical platform to probe the interactions between a model lipid bilayer and TEVs. Possible applications of this technology may be found in biomedical diagnostics, where studying the efficacy of treatments in hampering the effects of cancer are of interest.

1.2. Project Description

The scope of this project can be framed within the context of developing a biomimetic electronic platform with a model lipid bilayer as a surface functionalization layer for the analysis of interactions with TEVs. This section describes the steps necessary to characterize and optimize

this platform. The experimental portion of this thesis is highlighted as contributions to some of these steps.

To successfully develop this platform a multi-component plan has previously been developed by the Daniel Lab and collaborators. The projected milestones needed before conducting mechanistic analyses of TEV mediated processes on the electrical platform are:

1. Collect and characterize TEVs
2. Conduct and analyze the behavior of cells infected with TEVs
3. Make and optimize SLBs on OECTs (SLB-OECT platform)
4. Perform electrical TEV characterizations on OECTs
5. Characterize electrical outputs of cells infected with TEVs on OECTs

The work of this thesis is centered on the characterization of TEVs and analyzing their effect on cells (Fig. 1.1). Briefly, model epithelial cells were infected with TEVs and observed to show the ability of TEVs to promote angiogenesis, the formation of new vasculature. Furthermore, a method to block the behavior of TEVs was also explored. Taken together these studies allowed questions like “How long after exposure to TEVs will cells display signs of malignancy?” and “Can the effects of TEV exposure be eluded?” to be answered.

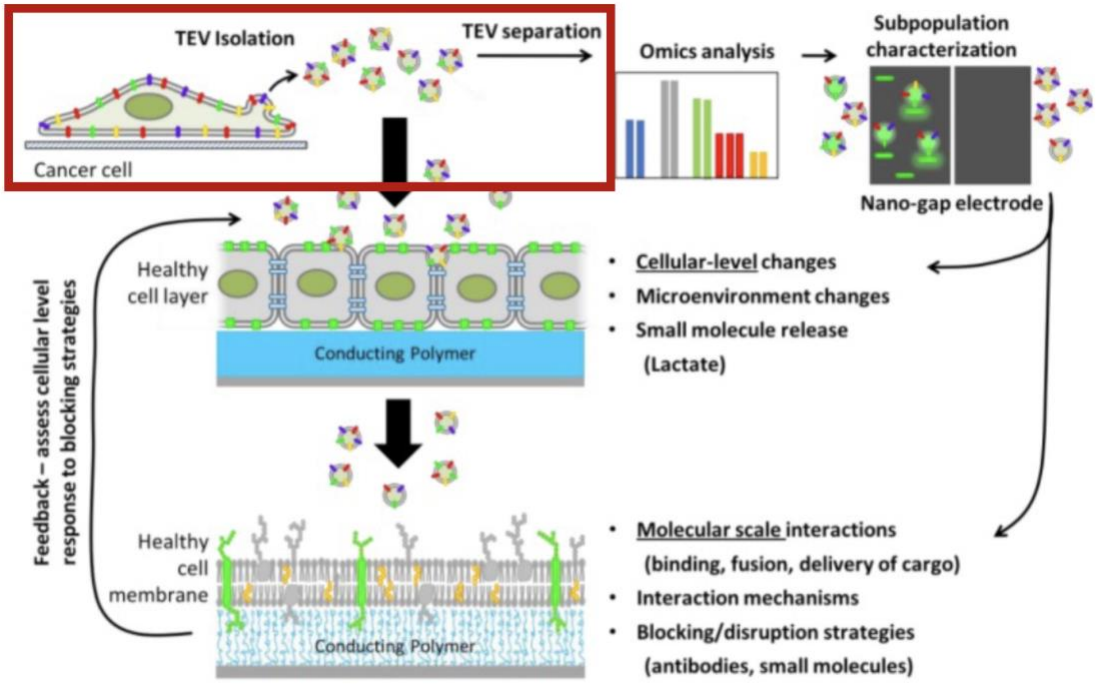

Figure 1.1. Flow Tasks for the Overall SLB-OECT Project. The project road map for the SLB-OECT platform. The boxed portion indicates the areas of contribution outlined in this thesis.

The data obtained in these studies will be leveraged to understand and optimize the readouts of the TEVs and TEV-infected cells on OECT only devices in milestones 4 and 5. Moreover, the observations from each of these milestones will not only inform the design and subsequent improvements of the SLB-OECT device itself, but also the TEV analyses to be conducted using the SLB-OECT device.

1.3. Future Applications

The work described in this thesis will serve as preliminary results for the SLB-OECT device being developed. The outcomes observed here provide baseline data for this same subset of experiments to be carried out on both OECTs and the model SLB-OECT platform. If successful, this device has immediate applications in screening drugs, to characterize their interactions with cellular membranes, and personalized medicine, as patient samples could be collected, purified,

and examined for certain biomarkers. This device also opens the potential for use in studies seeking to explore and characterize TEV effects on other cell types not explored in these studies. Moreover, this device can also be used to characterize the pathological mechanisms of other diseases, outside of cancer, that act on membranes.

1.4. Conclusions

Overall, the experimental work presented in this thesis represents a contribution to important innovations in the deposition and characterization of SLBs for biosensing and cancer diagnostic applications. Although model lipid membranes used in neuronal, immune, and other cell studies are reviewed for preparation and characterization methods employed, they serve as examples of the versatility and potential of this platform.

1.5. References

1. Dillekås, H., Rogers, M. S. & Straume, O. Are 90% of deaths from cancer caused by metastases? *Cancer Med.* **8**, 5574–5576 (2019).
2. Gupta, G. P. & Massagué, J. Cancer Metastasis: Building a Framework. *Cell* vol. 127 679–695 (2006).
3. Lei, X. *et al.* Immune cells within the tumor microenvironment: Biological functions and roles in cancer immunotherapy. *Cancer Lett.* **470**, 126–133 (2020).
4. Scioli, M. G. *et al.* Adipose-derived stem cells in cancer progression: New perspectives and opportunities. *Int. J. Mol. Sci.* **20**, (2019).
5. Hui, L. & Chen, Y. Tumor microenvironment: Sanctuary of the devil. *Cancer Letters* vol. 368 7–13 (2015).
6. Wang, M. *et al.* Role of tumor microenvironment in tumorigenesis. *Journal of Cancer* vol. 8 761–773 (2017).
7. Karnoub, A. E. *et al.* Mesenchymal stem cells within tumour stroma promote breast cancer metastasis. *Nature* **449**, 557–563 (2007).
8. Lin, W. & Karin, M. A cytokine-mediated link between innate immunity , inflammation , and cancer Find the latest version : Review series A cytokine-mediated link between innate immunity , inflammation , and cancer. *J. Clin. Invest.* **117**, 1175–1183 (2007).
9. Takebe, N., Warren, R. Q. & Ivy, S. P. Breast cancer growth and metastasis: Interplay between cancer stem cells, embryonic signaling pathways and epithelial-to-mesenchymal transition. *Breast Cancer Res.* **13**, (2011).
10. Liotta, L. A. & Kohn, E. C. The microenvironment of the tumour - Host interface. *Nature* **411**, 375–379 (2001).
11. Tkach, M. & Théry, C. Communication by Extracellular Vesicles: Where We Are and Where We Need to Go. *Cell* **164**, 1226–1232 (2016).
12. Colombo, M., Raposo, G. & Théry, C. Biogenesis, Secretion, and Intercellular Interactions of Exosomes and Other Extracellular Vesicles. *Annu. Rev. Cell Dev. Biol.* **30**, 255–289 (2014).
13. Kowal, J. *et al.* Proteomic comparison defines novel markers to characterize heterogeneous populations of extracellular vesicle subtypes. *Proc. Natl. Acad. Sci.* **113**, E968–E977 (2016).

14. Skog, J. *et al.* Glioblastoma microvesicles transport RNA and proteins that promote tumour growth and provide diagnostic biomarkers. *Nat. Cell Biol.* **10**, 1470–1476 (2008).
15. Fujita, Y., Yoshioka, Y. & Ochiya, T. Extracellular vesicle transfer of cancer pathogenic components. *Cancer Sci.* **107**, 385–390 (2016).
16. Sun, Z. *et al.* Emerging role of exosome-derived long non-coding RNAs in tumor microenvironment. *Mol. Cancer* **17**, 1–9 (2018).
17. Costa-silva, B. *et al.* Pancreatic cancer exosomes initiate pre-metastatic niche formation in the liver Bruno. *Nat Cell Biol* **17**, 816–826 (2018).
18. Han, L., Lam, E. W. F. & Sun, Y. Extracellular vesicles in the tumor microenvironment: Old stories, but new tales. *Mol. Cancer* **18**, 1–14 (2019).
19. Camussi, G. *et al.* Exosome/microvesicle-mediated epigenetic reprogramming of cells. *Am. J. Cancer Res.* **1**, 98–110 (2007).
20. Zomer, A. *et al.* In vivo imaging reveals extracellular vesicle-mediated phenocopying of metastatic behavior. *Cell* **161**, 1046–1057 (2015).
21. Ridder, K. *et al.* Extracellular Vesicle-Mediated Transfer of Genetic Information between the Hematopoietic System and the Brain in Response to Inflammation. *PLoS Biol.* **12**, 1001874 (2014).
22. Lai, C. P. *et al.* Dynamic biodistribution of extracellular vesicles in vivo using a multimodal imaging reporter. *ACS Nano* **8**, 483–494 (2014).
23. Lai, C. P. *et al.* Visualization and tracking of tumour extracellular vesicle delivery and RNA translation using multiplexed reporters. *Nat. Commun.* **6**, 1–12 (2015).
24. Uribe, J. *et al.* A supported membrane platform to assess surface interactions between extracellular vesicles and stromal cells. *ACS Biomater. Sci. Eng.* acsbiomaterials.0c00133 (2020) doi:10.1021/acsbiomaterials.0c00133.
25. Ghosh Moulick, R. *et al.* Reconstitution of Fusion Proteins in Supported Lipid Bilayers for the Study of Cell Surface Receptor-Ligand Interactions in Cell-Cell Contact. *Langmuir* **32**, 3462–3469 (2016).
26. Pautot, S., Lee, H., Isacoff, E. Y. & Groves, J. T. Neuronal synapse interaction reconstituted between live cells and supported lipid bilayers. *Nat. Chem. Biol.* **1**, 283–289 (2005).
27. Thid, D. *et al.* Supported phospholipid bilayers as a platform for neural progenitor cell

culture. *J. Biomed. Mater. Res. Part A* **84A**, 940–953 (2008).

28. Afanasenkau, D. & Offenhäusser, A. Positively Charged Supported Lipid Bilayers as a Biomimetic Platform for Neuronal Cell Culture. *Langmuir* **28**, 13387–13394 (2012).
29. Richards, M. J. *et al.* Membrane Protein Mobility and Orientation Preserved in Supported Bilayers Created Directly from Cell Plasma Membrane Blebs. *Langmuir* **32**, 2963–2974 (2016).
30. Hsia, C. Y., Chen, L., Singh, R. R., DeLisa, M. P. & Daniel, S. A Molecularly Complete Planar Bacterial Outer Membrane Platform. *Sci. Rep.* **6**, 1–14 (2016).
31. Rivnay, J. *et al.* Organic electrochemical transistors for cell-based impedance sensing. *Appl. Phys. Lett.* **106**, 43301 (2015).
32. Yeung, S. Y., Gu, X., Tsang, C. M., Tsao, S. W. & Hsing, I. ming. Engineering organic electrochemical transistor (OECT) to be sensitive cell-based biosensor through tuning of channel area. *Sensors Actuators, A Phys.* **287**, 185–193 (2019).
33. Strakosas, X., Bongo, M. & Owens, R. M. The organic electrochemical transistor for biological applications. *Journal of Applied Polymer Science* vol. 132 41735 (2015).
34. Su, H. *et al.* Facile Generation of Biomimetic-Supported Lipid Bilayers on Conducting Polymer Surfaces for Membrane Biosensing. *ACS Appl. Mater. Interfaces* **11**, 43799–43810 (2019).
35. Liu, H. Y. *et al.* Biomembrane-based organic electronic devices for ligand–receptor binding studies. *Anal. Bioanal. Chem.* **412**, 6265–6273 (2020).
36. Liu, H. Y. *et al.* Self-Assembly of Mammalian-Cell Membranes on Bioelectronic Devices with Functional Transmembrane Proteins. *Langmuir* **36**, 7325–7331 (2020).
37. Pappa, A. M. *et al.* Optical and electronic ion channel monitoring from native human membranes. *ACS Nano* **14**, 12538–12545 (2020).

Chapter 2: Background

2.1. Introduction

This chapter aims to contextualize and motivate the methods to be used for the SLB portion of the SLB-OECT platform to be optimized following this work. First, is a brief description of the functionalization methods commonly used in SLB studies. This will be followed by a review of relevant studies utilizing the SLB platform for cell culture studies. Finally, important outcomes from the reviewed literature will be summarized. The in-depth review will be split into two subsections: compositional functionalization and physiological functionalization. As previously mentioned, SLBs have emerged as a model membrane system to study key cellular interactions on a molecular level. The studies seeking to employ SLB technology typically aim to investigate the role of proteins, peptides, and other molecules in cell behavior through the incorporation of bioactive molecules of interest into the bilayer, or they will tune the SLBs to investigate how physiological conditions affect cell behavior. The second method will typically involve the study of mechanistic factors or environmental conditions to best replicate a cell's microenvironment in vivo and identify preferential or adverse conditions that may serve as biomarkers or indicators of key biological processes. Here the conjugation of ECM molecules and optimization of surface electrostatics will be reviewed as the SLB-OECT system will need to capitalize on the foundational knowledge gained from these compositional and physiological studies, respectively.

2.2. Review of Literature

This section is a review of the literature necessary to both contextualize the project and identify the potential areas in which this project can be applied. This review section will be presented in the following subsections to highlight some of the methods employed in SLB studies and the circumstances in which these methods were most useful:

- 2.2.1. Bilayer Functionalization Methods
- 2.2.2. ECM Molecule Functionalization of Supported Lipid Bilayers
- 2.2.3. Surface Electrostatic Functionalization of Supported Lipid Bilayers

2.2.1. Bilayer Functionalization Methods

There are several well-studied methods to deposit SLBs on surfaces including Langmuir-Blodgett[1,2]/Langmuir-Schaffer deposition[3], vesicle fusion[4], and solvent-assisted lipid bilayer (SALB) formation[5]. These methods can be used separately or jointly, and they each have intrinsic advantages or disadvantages, making their uses contingent upon the intended application. Below, brief descriptions of each deposition technique are provided.

Langmuir-Blodgett/Langmuir-Schaffer deposition

The Langmuir-Blodgett (LB) method, which originated in 1917, is a means of transferring a floating monolayer from water or buffer surfaces to a solid substrate by vertically dipping or pulling the substrate perpendicular to the deposition medium's surface[2] (Fig. 2.1a). The substrate can also be dipped repeatedly to make multilayer films[1]. With this method, the monolayer floating on the air-water interface must be an amphiphile, such as a fatty acid or phospholipid, and in the case of SLBs, the substrate surface must be hydrophilic. Once the substrate is drawn through the medium's surface, the monolayer is transferred with the hydrophilic headgroup facing the substrate. To make a bilayer, the substrate, containing the already LB deposited monolayer with hydrophobic tail groups sticking out, is then horizontally dipped onto the deposition medium in what is referred to as the Langmuir-Schaefer (LS) method[3]. As seen in Figure 2.1b this transfers the upper leaflet of the bilayer where the hydrophobic tail groups of both leaflets face each other, and the hydrophilic headgroups face the substrate and the environment. Key advantages to this

method are precise control over surface pressure and monolayer thickness[6] as well as the ability to deposit asymmetric bilayers[7] where the composition of the leaflets are different. An inherent disadvantage of this method, however, is the difficulty incorporating proteins onto the monolayers. In some applications, exposure of samples to air can lead to the denaturing of the proteins requiring additional measures to be taken to successfully incorporate active proteins.

Vesicle Fusion

Many SLB studies use vesicle fusion, a method developed by the McConnell laboratory in the 1980s[4,8], to prepare bilayers because of its simplicity and accessibility. In this method, sonicated vesicles in aqueous suspension spontaneously adsorb and fuse with an appropriately cleaned surface to form a continuous bilayer[9] (Fig 2.1c). The fusion process is reliant on the instability of vesicles interacting with the substrate surface, and the surface tension between the vesicles and the surface to promote vesicle rupture and spontaneous SLB formation[10,11]. Outside of its convenience, a key advantage of this method is its versatility in lipid composition and protein/peptide conjugation methods. Through this method, biomolecules of interest can be incorporated into the bilayer in vesicular form to create complex SLBs that can be varied by composition, surface charge, fluidity, etc. Hybrid SLBs that incorporate native plasma cell membrane material while preserving the original orientation and function of the membrane proteins through cell blebs also utilize this method to form highly complex SLBs without the need for protein conjugation[12–14]. The versatility of this method can also be a restriction, however, as increasing SLB complexity also increases the factors that may affect, and even prevent, successful vesicle adsorption and fusion. These factors include vesicle composition, size, solution pH, surface cleanliness, and charge to name a few[15,16]. Furthermore, SLB formation via vesicle fusion does not

readily facilitate the formation of asymmetric bilayers unless combined with a Langmuir deposition method.

Solvent-Assisted Lipid Bilayer (SALB) Formation

Inspired by the well-studied fact that phospholipids can self-assemble in certain solvent environments, a solvent-exchange process was developed in 2010 where lipids in a pure organic solvent (isopropanol) were incubated with a solid support, and aqueous buffer solution was gradually introduced, step-by-step, to induce a series of phase transitions from inverted micelles to lamellar-phase lipid bilayers[17]. Expanding upon this protocol, Tabei et al. introduced the SALB method which completes the aforementioned solvent exchange from pure organic solvent to aqueous buffer in just one step so that an SLB can be quickly formed[18] (Fig 2.1d). Two principal advantages of this approach are the increased versatility in lipid assemblies and bilayer supports, bypassing the need for vesicle preparation and expanding the capabilities of SLB formation to materials otherwise unsuitable when using vesicle fusion and Langmuir methods[19–21]. At the same time, extreme care is needed during the washing step of this method as solvent can easily be left behind leading to the denaturing of proteins over time[22,23]. There is also a limitation as larger proteins denature in solvent making this method unfitting for those studies[24].

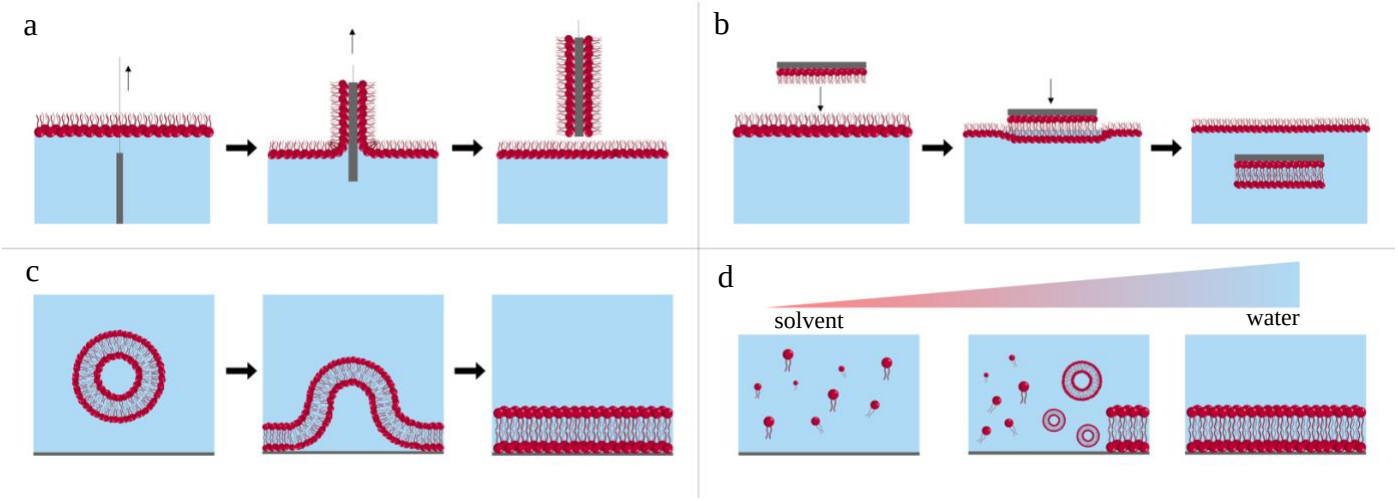

Figure 2.1 SLB Formation methods. A) Langmuir-Blodgett method involves the dipping or pulling of a substrate through a monolayer on the water-air interface. B) Langmuir-Schaefer method requires the substrate containing a LB deposited monolayer to be horizontally dipped onto the deposition medium to form a bilayer. C) Vesicle fusion involves the spontaneous adsorption, rupture, and fusion of a vesicle to a substrate's surface. D) SALB formation occurs in a single step through the exchange from organic solvent to an aqueous buffer. During this step, the initial phospholipids go through phase changes to eventually self-assemble into a bilayer.

2.2.2 ECM Molecule Functionalization of Supported Lipid Bilayers

The proteins within the extracellular matrix (ECM) have long been recognized for their central roles in cell adhesion, and subsequently, proliferation and differentiation. In studies that seek to investigate cell-ECM interfaces, these roles have been exploited in vitro to facilitate cell adhesion to ECM protein-coated synthetic surfaces. One major challenge, however, to using traditional culture surfaces like glass or polystyrene, is their facilitation of non-specific protein adsorption which hinders studies seeking to study the correlation between cells and specific ECM components. In response to this, targeted cell-matrix interaction studies have capitalized on the anti-fouling properties of SLBs to conduct their investigations while eluding the risks of misleading cellular responses promoted by non-targeted proteins.

Collagen type I (Col I) and fibronectin (FN) are major ECM proteins most often implored in cell studies. They are both widely known for their vast abundance throughout the body and

ability to provide structural and biochemical support to surrounding cells. In SLB studies, Col I and FN can be coupled to or inserted into the SLBs to evaluate cellular responses to these proteins. In the earliest example, Col I was covalently bound to POPC bilayers functionalized with NHS-activated DP-NGPE to investigate smooth muscle cell (A10) behavior. To do this, Col I was conjugated on POPC/NGPE bilayers through amide bond formation where primary amine groups of Col I reacted with DP-NGPE. The bound collagen molecules were then able to interact with integrin receptors on the A10 cell surface to facilitate successful cell culture unlike bare POPC and POPC/NGPE SLBs without Col I. This method also allowed control over the binding capacity of Col I within the SLB through the variation of NHS DP-NGPE molar fraction. Thus, offering the ability to potentially investigate cellular response to both specific ECM molecules and biophysical cues like fluidity and ligand density[25].

Following this work, studies adopting this method sought to further investigate cell growth and response to more complex systems of conjugated proteins. In one such study by the same group, NIH 3T3 cells were cultured on Col I, FN, or combined Col I-FN conjugated bilayers and compared in parallel to cells on oxygen plasma-treated polystyrene (PSo) surfaces coated with the same proteins. For SLBs containing both proteins, Col I was covalently bound via the aforementioned amine coupling chemistry followed by the adsorption of FN through presumed Col I-FN binding domains. Cell counts and spreading areas were observed to be highest on both the combined Col I-FN and FN only SLBs compared to both Col I only SLBs and PSo surfaces. Furthermore, immunofluorescent data revealed that the NIH 3T3 cells were able to remodel their microenvironment by secreting FN on PSo surfaces likely explaining the insignificant differences in cell behavior across all protein-coated and non-coated PSo surfaces[26]. This endogenous FN expression caused by NIH 3T3 secretion was only minimally seen on Col I SLBs though,

presumably due to the anti-fouling nature of the SLBs used, highlighting their ability to circumvent unwanted cell remodeling. This study also identified a potential preference or necessity of FN to mediate NIH3T3 cell adhesion. In another study, Col I or FN were covalently bound to DOPC/NGPE bilayers formed via the SALB formation method. As previously mentioned, the SALB method of formation allows for bilayer formation on substrates otherwise obstinate to the commonly used vesicle fusion method. This formation method coupled with amide chemistry enabled protein conjugation to SLBs on SiO2 substrates. When compared to protein-coated SiO2 surfaces, Col I and FN on SLBs displayed higher structural flexibility and greater surface binding efficiencies. In addition, cell adhesion and proliferation trends were enhanced on SLBs despite greater protein coverage on SiO2 surfaces due to nonspecific adsorption suggesting a correlation between the improved biological activity of Col I and FN within the SLBs and cell behavior[27].

In an effort to develop a platform that more closely mimics the compositional complexity of the ECM, an SLB was functionalized with decellularized extracellular matrix (dECM) extracted from mouse adipose tissue. dECM components, decellularized via chemical/enzymatic treatments, were covalently attached to DOPC/NGPE bilayers through amine coupling chemistry[28]. A key benefit of this method is the dECM's ability to retain its natural ultrastructure and protein compositions. Therefore, attaching dECM components to SLBs enabled the investigation of cellular response to native ECM constituents like collagen, fibronectin, and glycosaminoglycans (GAGs) in a manner that had yet to be explored. This platform not only supported Huh 7.5 cell attachment and proliferation but also promoted albumin production – a cellular function mediated by cell-ECM interactions[28]. While this study is currently the only of its kind, the dECM-SLB's ability to mimic both the mechanical and complex biochemical properties of the native ECM will

likely garner much attention for future studies seeking to investigate whole ECM-mediated responses.

Although the direct conjugation of proteins to SLBs offers a more realistic representation of the ECM, risks of pathogen transfer or adverse immune reactivity, from proteins derived from xenografts or cadavers, or general instability caused by denaturation or batch-to-batch variability before SLB conjugation can cause limitations in long-term studies[29–32]. Peptide-associated bilayers are commonly employed to elude these risks while still mimicking the bioactivity of parent ECM proteins via specific recognition by integrins on cell membranes. Furthermore, the precise control over ligand density and orientation enabled through the use of short peptides is likely an appealing feature for studies seeking to connect cellular responses to specific biological events or conditions. Many strategies have been implored to conjugate peptides to SLBs. In one such method, bioactive peptide sequences are conjugated with hydrophobic tails via spacer groups to create peptide amphiphiles (PAs). The tails of the PAs enable spontaneous self-association with equally hydrophobic lipids to form vesicles for bilayer formation. In one study using this method, mouse fibroblast (L-Cells) cell behavior was observed on bilayers functionalized with two RGD-containing peptide amphiphiles: shorter (C16)2-Glu-C2-GRGDSP or longer (C16)2-Glu-PEO-GRGDSP[33]. The tri-amino acid sequence arginine-glycine-aspartate (RGD) is a ubiquitous integrin-binding domain found in several ECM proteins. Extensive research has shown RGD's ability to engage several integrin species and established the efficiency in which RGD-containing peptides can promote cell adhesion to several substrates[34,35]. Along this line, this study and many others have functionalized SLBs with RGD peptides to analyze cell adhesion, proliferation, and viability[36–40]. The results of this study showed fibroblast adhesion was only successful on SLBs functionalized with the larger (PEO) amphiphile suggesting the presence of RGD alone is not

sufficient to promote cell adhesion. Instead, peptide presentation and accessibility may be equally as important as seen by the inability of cells to adhere to SLBs functionalized with the shorter (C2) amphiphile[33].

Another study observing adult hippocampal neural stem cell (NSC) behavior on PA SLBs functionalized with longer GGGNGEPRGDTYRAY derived from bone sialoprotein (bsp-RGD(15)) or shorter GRGDSP derived from fibronectin yielded similar results. Although NSCs were able to successfully attach, proliferate, and differentiate on all tested surfaces, cells on GRGDSP SLBs appeared loosely attached and aggregated compared to the monolayer of cell attachment observed on bsp-RGD(15) SLBs and control laminin surfaces. This difference in attachment between SLBs was attributed to PA conformation in which the increased flexibility of longer bsp-RGD(15) likely promoted a 'looped' peptide presentation[29]. Previous studies have shown the structure of RGD to influence cell behavior with looped or cyclic peptides selectively recruiting different integrins on cell surfaces than linear peptides[41–43]. To illustrate this, cell attachment to bsp-RGD(15) has been found to be mediated by αvβ3 integrins[44]. Furthermore, cyclic or looped peptides exhibit a higher affinity for the αvβ3 compared to linear peptides, supporting the presumption of bsp-RGD(15)'s looped conformation and illuminating a likely cause for reduced adhesion on SLBs containing linear GRGDSP[45,46]. By conjugating RGD peptides of varying lengths and conformations with SLBs, researchers can effectively dissect the role of specific ECM ligand-receptor interactions on the behavior of cells.

An alternative peptide conjugation method is through covalent coupling. Studies using IKVAV, another well-known binding motif derived from laminin, utilize terminal cysteines to bind IKVAV containing peptides to thiol-reactive maleimido lipids in the bilayer. Svedhem et. al investigated the performance of SLBs containing synthetic 19-mer IKVAV-containing peptide

(CS- RARKQAASIKVAVSADR) in model neuronal PC-12 cell studies and found the platform to be successful[47]. Following this work, Thid et al. investigated adult hippocampal progenitor (AHP) behavior on IKAVAV functionalized bilayers. Their results elucidated a dependence of AHP attachment on the density of IKVAV peptides tethered to the SLB and proved AHP recognition of IKVAV is specific as cells did not adhere to bilayers conjugated with peptides containing the scrambled IKVAV sequence, VKAIV[48]. However, long-term studies also revealed cells grew in clusters forming networks of 3D colonies instead of monolayer-like growth seen on the laminin-coated control surfaces. This behavior was attributed to the depletion of available ligand attachment sites within the bilayer due to the early recruitment of laterally mobile peptides by initially seeded cells causing newly developed cells to adhere to ligands on the surfaces of adjacent cells [48]. Future studies seeking to overcome this may be able to employ methods to reduce the lateral translocation of the ligands to decrease the amount of ligand depletion within the bilayers as cells may not be able to recruit ligands as easily.

2.2.3. Surface Electrostatic Functionalization of Supported Lipid Bilayers

A basic requirement for any cell culture platform is its ability to promote cellular attachment. Accordingly, the electrostatic functionalization of cell culture substrates with materials that can interact with the negatively charged cell membrane has been widely used to study cell adhesion and neuronal processes. Coating surfaces with positively charged materials such as poly-l-lysine (PLL) and polyethyleneimine (PEI) enhances the adhesion capabilities of cells with known weak adhesion properties while also removing the need for additional adhesion molecules[49,50]. Furthermore, neurons and neurites have been repeatedly shown to preferentially adhere to and form on positively charged surfaces over native ECM proteins as was the case in cell patterning studies in which glass and other substrates were co-coated with charged materials and ECM protein laminin[51,52]. This improved attachment, however, limits the capacity for studying

the role of electrostatics in cell migration and differentiation as cells were postulated to be resistant to changing positions or migrating following deposition onto positively charged surfaces[51]. To further investigate the role of electrostatics on cell behavior and overcome this barrier of immobility, it is valuable to utilize the biomimetic and fluidic nature of SLBs to induce functional cellular processes.

As previously mentioned, SLBs composed of zwitterionic lipids such as POPC carry a neutral charge preventing nonspecific, electrostatic interactions from occurring with charged cell membranes[53–55]. One way to overcome this is through mixed lipid bilayers. In this method, cationic or anionic lipids are integrated into neutrally charged SLBs at varying concentrations. Similar to results yielded from the aforementioned substrates, the addition of positively charged lipids like 1,2-dioleoyl-3-trimethylammonium-propane (DOTAP) improved neuronal cell attachment compared to POPC-only SLBs[55,56]. When compared to control PLL coated glass, positively charged DOTAP SLBs also displayed comparable neuronal cell attachment with pure DOTAP SLBs attachment surpassing the PLL control. However, cell proliferation and bilayer diffusivity of purely cationic SLBs were found to be low with overall best performance occurring in partially cationic bilayers containing 30% positively charged lipids[55,56]. This finding suggests charge density to be an additional parameter impacting cell behavior on SLBs. Additionally, a threshold for ideal charged lipid densities required for optimum cell attachment, cell proliferation, and SLB functionality could potentially be identified through further investigation.

Due to the highly tunable nature of SLBs, there are a number of potential explanations for the depreciating results reported as charge density increases. First, lipid headgroup interactions might fuse the bilayer together[57,58]. Studies revealed the headgroup for some cationic lipids and the negative end of zwitterionic lipids headgroup lie within the same plane enabling potential

electrostatic interactions between headgroups thereby slowing the mobility of the SLB. In addition, the electrostatic repulsion between lipid molecules of similar charge may suppress diffusivity in SLBs of higher cationic concentration[59]. The suggested decreases in cell proliferation while still yielding increased cell attachment implies a mobility problem similar to the coated static substrates mentioned early on. Therefore, the reported decrease in bilayer diffusivity is a likely contributor as fluidity has been proven to be a necessary component in these studies. Lastly, the purely cationic SLBs are likely to generate strong interactions with the negative cell membranes rendering the cells once again unwilling to migrate. Identifying and maintaining the charge density threshold for charged lipids within SLBs will help to preserve a physiologically relevant model.

In biosensing studies, a major challenge is the restriction on support materials suitable for bilayer formation as metals and other conducting materials require additional surface modifications to promote the rupture and fusion of vesicles in order to properly form bilayers. Currently, chemical modifications such as the use of thiol either in thiol labeled lipids or thiol self-assembled monolayers are employed to adjust surface hydrophilicity. However, these modifications have been found to affect the electric and dynamic response of bilayers impeding the electrical and optical signals necessary for these studies. To overcome this, Choi et al. used varied ratios of POPC and positively charged DOTAP on negatively charged gold substrates to promote an attractive electrostatic interaction that was strong enough to induce vesicle rupture and, therefore, bilayer formation[56]. The use of electrostatics as a means to physiologically provoke bilayer formation without additional surface modifications was also coupled with previous knowledge of the suitability of positively charged bilayers for cell adhesion and proliferation to demonstrate the capabilities of gold-supported bilayers in long-term neuronal cell studies. With positively charged PDL film on the gold substrate taken as a control, viability and morphology of

primary neuronal cells on mixed lipid SLBs on gold were similar to the conventional control group. Moreover, POPC-only SLBs inhibited cellular attachment on the gold substrates further proving the importance of surface charge on cell adhesion[56].

These mixed lipid electrostatic systems can also be used to optimize protein and peptide-associated bilayers, offering the potential to enhance protein/peptide-specific studies. For example, at physiological pH, most biomolecules bear an overall positive or negative charge, so the incorporation of oppositely charged lipids could improve the protein/peptide-lipid association. Demonstrating this, Travaglia et al. introduced an approach to associate the nerve growth factor peptide sequence, NGF(1–14), with lipid vesicles using an electrostatic model. In this proof-of-concept study, negatively charged 1-palmitoyl-2-oleoyl-sn-glycero-3-phospho-L-serine (POPS) lipids were mixed with POPC to attract positively charged NGF(1-14). 24hr incubation of Human neuroblastoma (SH-SY5Y) cells showed improved cell adhesion and proliferation on the POPS-NGF bilayer compared to the POPC-NGF bilayer[60]. Similarly, retinal microvascular endothelial cells (ECs) were cultured on mixed bilayers containing varying ratios of POPC and cationic 1-palmitoyl-2-oleoyl-sn-glycero-3-ethylphosphocholine (POEPC). These SLBs were then further functionalized with negatively charged ferritin. Similar to the results of the electrostatic studies by Choi and Afanasenkau mentioned earlier, EC attachment improved as the concentration of POEPC increased with optimum cell performance on EPC25 SLBs containing 25% POEPC. Once functionalized with ferritin, EC viability improved across all platforms including mostly zwitterionic EPC5 SLBs made of 5% POEPC which did not adequately support cell adhesion prior to ferritin functionalization. Furthermore, ferritin further enhanced adhesion and proliferation on EPC25 SLBs compared to both the charged EPC25 SLBs and ferritin-only SLBs yielding the highest cell number and proliferation values of all platforms within the study[61]. These results along

with Travalia et al's findings allude to the synergistic nature of this predominantly electrostatic method of association being an enhancing factor to cell behavior and response to these platforms.

Although the use of polyelectrolyte multilayer (PEM) films is still fairly underexplored in bilayer-associated cell culture studies, PEM films are a versatile tool for investigating the role of electrostatic interactions in traditional cell culture studies. By varying electrolyte composition and assembly conditions, this method offers the potential to regulate properties, such as surface topography, surface charge, and stiffness, all of which may alter cell adhesion, protein adsorption, and cell differentiation[62]. In this method, films constructed from charged materials such as native polypeptides, poly-L-lysine (PLL), poly-L-glutamic acid (PLGA), hyaluronic acid, and chitosan can be deposited onto the SLBs to produce layered microenvironmental substrates. This system is characterized by the electrostatic interactions established when oppositely charged layers are adsorbed onto one another to not only promote electrostatic attraction amongst layers but also between the uppermost layer and seeded cell membranes. Lee et al. investigated the effects of SLBs with adsorbed PEM films on adhesion and differentiation of neural stem/progenitor cells (NSPCs). Short-term cell culture studies showed PEM-SLBs with polycation PLL as the terminal film layer induced differentiation into functional neurons, strong axonal growth, and synaptogenesis compared with those on PEM-SLBs with polyanion PLGA as the terminal film layer[63]. Additionally, cell performance was enhanced as the number of layers increased predictably due to the decrease in stiffness observed with the addition of each layer as neurons are known to favor softer substrates. The ability to simultaneously adjust surface charge and stiffness within SLBs will allow the relationship between electrostatics and mechanics to be investigated in parallel.

2.3. Summary of Background

The preceding was a brief review of examples from literature where SLBs were used as cell culture platforms and the methods taken by various groups to functionalize these bilayers, usually to promote cell adhesion and observe cellular response to these functionalization methods. These applications exemplify only a snapshot of the breadth of interactions that are mediated by SLBs and showcase a few of the areas in which the SLB-OECT platform could be of future use. Various existing techniques for depositing lipid bilayers on various substrates were also reviewed. These techniques are based on either the spontaneous self-assembly of bilayers through vesicles or organic solvents, or on Langmuir trough deposition. The SLB-OECT to be optimized following the work of this thesis focuses on vesicle fusion as the SLBs to be deposited on the OECT devices will be derived from cell blebs to form SLBs that closely mimic the native cell membrane. The lessons learned from literature will be used to inform and further optimize the protocols to functionalize the SLB-OECT platform.

2.4. References

1. Blodgett, K. B. Films Built by Depositing Successive Monomolecular Layers on a Solid Surface. *J. Am. Chem. Soc.* **57**, 1007–1022 (2002).
2. Langmuir, I. THE CONSTITUTION AND FUNDAMENTAL PROPERTIES OF SOLIDS AND LIQUIDS. II. LIQUIDS.1. *J. Am. Chem. Soc.* **39**, 1848–1906 (2002).
3. Langmuir, I. & Schaefer, V. J. Activities of Urease and Pepsin Monolayers. *Trans. Faraday Soc* **33**, 17 (1937).
4. Tamm, L. K. & McConnell, H. M. Supported phospholipid bilayers. *Biophys. J.* **47**, 105–113 (1985).
5. Tabaei, S. R., Choi, J. H., Haw Zan, G., Zhdanov, V. P. & Cho, N. J. Solvent-assisted lipid bilayer formation on silicon dioxide and gold. *Langmuir* **30**, 10363–10373 (2014).
6. Langmuir Films - Nanoscience Instruments. https://www.nanoscience.com/techniques/langmuir-films/.
7. Sanderson, J. M. Resolving the kinetics of lipid, protein and peptide diffusion in membranes. *Mol. Membr. Biol.* **29**, 118–143 (2012).
8. McConnell, H. M., Watts, T. H., Weis, R. M. & Brian, A. A. Supported planar membranes in studies of cell-cell recognition in the immune system. *Biochim. Biophys. Acta - Rev. Biomembr.* **864**, 95–106 (1986).
9. Kalb, E., Frey, S. & Tamm, L. K. Formation of supported planar bilayers by fusion of vesicles to supported phospholipid monolayers. *Biochim. Biophys. Acta - Biomembr.* **1103**, 307–316 (1992).
10. and, P. S. C. & Boxer*, S. G. Formation and Spreading of Lipid Bilayers on Planar Glass Supports. *J. Phys. Chem. B* **103**, 2554–2559 (1999).
11. Biswas, K. H., Jackman, J. A., Park, J. H., Groves, J. T. & Cho, N.-J. Interfacial Forces Dictate the Pathway of Phospholipid Vesicle Adsorption onto Silicon Dioxide Surfaces. *Langmuir* **34**, 1775–1782 (2018).
12. Richards, M. J. *et al.* Membrane Protein Mobility and Orientation Preserved in Supported Bilayers Created Directly from Cell Plasma Membrane Blebs. *Langmuir* **32**, 2963–2974 (2016).
13. Hsia, C. Y., Chen, L., Singh, R. R., DeLisa, M. P. & Daniel, S. A Molecularly Complete Planar Bacterial Outer Membrane Platform. *Sci. Rep.* **6**, 1–14 (2016).

14. Uribe, J. *et al.* A supported membrane platform to assess surface interactions between extracellular vesicles and stromal cells. *ACS Biomater. Sci. Eng.* acsbiomaterials.0c00133 (2020) doi:10.1021/acsbiomaterials.0c00133.
15. Stelzle, M., Weissmuller, G. & Sackmann, E. On the Application of Supported Bilayers as Receptive Layers for Biosensors with Electrical Detection. *J. Phys. Chem* **97**, 2974–2981 (1993).
16. Erik Reimhult, *, Fredrik Höök, and & Kasemo, B. Intact Vesicle Adsorption and Supported Biomembrane Formation from Vesicles in Solution: Influence of Surface Chemistry, Vesicle Size, Temperature, and Osmotic Pressure†. *Langmuir* **19**, 1681–1691 (2002).
17. Hohner, A. O., David, M. P. C. & Rädler, J. O. Controlled solvent-exchange deposition of phospholipid membranes onto solid surfaces. *Biointerphases* **5**, 1 (2010).
18. Tabaei, S. R., Choi, J.-H., Zan, G. H., Zhdanov, V. P. & Cho, N.-J. Solvent-Assisted Lipid Bilayer Formation on Silicon Dioxide and Gold. *Langmuir* **30**, 10363–10373 (2014).
19. Jackman, J. A., Tabaei, S. R., Zhao, Z., Yorulmaz, S. & Cho, N.-J. Self-Assembly Formation of Lipid Bilayer Coatings on Bare Aluminum Oxide: Overcoming the Force of Interfacial Water. *ACS Appl. Mater. Interfaces* **7**, 959–968 (2014).
20. Jackman, J. A., Saravanan, R., Zhang, Y., Tabaei, S. R. & Cho, N.-J. Correlation between Membrane Partitioning and Functional Activity in a Single Lipid Vesicle Assay Establishes Design Guidelines for Antiviral Peptides. *Small* **11**, 2372–2379 (2015).
21. Ferhan, A. R. *et al.* Solvent-assisted preparation of supported lipid bilayers. *Nat. Protoc.* **14**, 2091–2118 (2019).
22. Jackman, J. A. & Cho, N.-J. Supported Lipid Bilayer Formation: Beyond Vesicle Fusion. *Langmuir* **36**, 1387–1400 (2020).
23. and, K. G. & Klibanov*, A. M. On Protein Denaturation in Aqueous−Organic Mixtures but Not in Pure Organic Solvents. *J. Am. Chem. Soc.* **118**, 11695–11700 (1996).
24. Kiessling, V., Yang, S. T. & Tamm, L. K. Supported Lipid Bilayers as Models for Studying Membrane Domains. *Curr. Top. Membr.* **75**, 1–23 (2015).
25. Huang, C.-J. *et al.* Type I Collagen-Functionalized Supported Lipid Bilayer as a Cell Culture Platform. doi:10.1021/bm901445r.
26. Huang, C.-J., Tseng, P.-Y. & Chang, Y.-C. Effects of extracellular matrix protein

functionalized fluid membrane on cell adhesion and matrix remodeling. (2010) doi:10.1016/j.biomaterials.2010.05.076.

27. Vafaei, S., Tabaei, S. R. & Cho, N. J. Optimizing the Performance of Supported Lipid Bilayers as Cell Culture Platforms Based on Extracellular Matrix Functionalization. *ACS Omega* **2**, 2395–2404 (2017).
28. Vafaei, S., Tabaei, S. R., Guneta, V., Choong, C. & Cho, N. J. Hybrid Biomimetic Interfaces Integrating Supported Lipid Bilayers with Decellularized Extracellular Matrix Components. *Langmuir* **34**, 3507–3516 (2018).
29. Ananthanarayanan, B., Little, L., Schaffer, D. V, Healy, K. E. & Tirrell, M. Neural stem cell adhesion and proliferation on phospholipid bilayers functionalized with RGD peptides. *Biomaterials* **31**, 8706–8715 (2010).
30. Bellis, S. L. Advantages of RGD peptides for directing cell association with biomaterials. (2011) doi:10.1016/j.biomaterials.2011.02.029.
31. Lebaron, R. G. & Athanasiou, K. A. Ex vivo synthesis of articular cartilage. *Biomaterials* **21**, 2575–2587 (2000).
32. Hubbell, J. A. Bioactive biomaterials. *Curr. Opin. Biotechnol.* **10**, 123–129 (1999).
33. Stroumpoulis, D., Haining, Z., Rubalcava, L., Gliem, J. & Tirrell, M. Cell adhesion and growth to peptide-patterned supported lipid membranes. *Langmuir* **23**, 3849–3856 (2007).
34. Ruoslahti, E. RGD AND OTHER RECOGNITION SEQUENCES FOR INTEGRINS. *http://dx.doi.org/10.1146/annurev.cellbio.12.1.697* **12**, 697–715 (2003).
35. U, H., C, D. & H, K. RGD modified polymers: biomaterials for stimulated cell adhesion and beyond. *Biomaterials* **24**, 4385–4415 (2003).
36. Verstappen, J. F. M. *et al.* RGD-functionalized supported lipid bilayers modulate pre-osteoblast adherence and promote osteogenic differentiation. *J. Biomed. Mater. Res. Part A* **108**, 923–937 (2020).
37. Zhu, X. *et al.* Cell adhesion on supported lipid bilayers functionalized with RGD peptides monitored by using a quartz crystal microbalance with dissipation. *Colloids Surfaces B Biointerfaces* **116**, 459–464 (2014).
38. Huth, M., Hertrich, S., Mezo, G., Madarasz, E. & Nickel, B. Neural stem cell spreading on lipid based artificial cell surfaces, characterized by combined X-ray and neutron reflectometry. *Materials (Basel).* **3**, 4994–5006 (2010).

39. Sandrin, L. *et al.* Cell adhesion through clustered ligand on fluid supported lipid bilayers. *Org. Biomol. Chem.* **8**, 1531–1534 (2010).
40. Kilic, A. & Kok, F. N. Peptide-functionalized supported lipid bilayers to construct cell membrane mimicking interfaces. *Colloids Surfaces B Biointerfaces* **176**, 18–26 (2019).
41. Pfaff, M. *et al.* Selective recognition of cyclic RGD peptides of NMR defined conformation by alpha IIb beta 3, alpha V beta 3, and alpha 5 beta 1 integrins. *J. Biol. Chem.* **269**, 20233–20238 (1994).
42. Pakalns, T. *et al.* Cellular recognition of synthetic peptide amphiphiles in self-assembled monolayer films. *Biomaterials* **20**, 2265–2279 (1999).
43. Ochsenhirt, S. E., Kokkoli, E., Mccarthy, J. B. & Tirrell, M. Effect of RGD secondary structure and the synergy site PHSRN on cell adhesion, spreading and specific integrin engagement. *Biomaterials* **27**, 3863–3874 (2006).
44. Rezania, A. & Healy, K. E. Integrin subunits responsible for adhesion of human osteoblast-like cells to biomimetic peptide surfaces. *J. Orthop. Res.* **17**, 615–623 (1999).
45. Xiao, Y. & Truskey, G. A. Effect of receptor-ligand affinity on the strength of endothelial cell adhesion. *Biophys. J.* **71**, 2869 (1996).
46. Verrier, S. *et al.* Function of linear and cyclic RGD-containing peptides in osteoprogenitor cells adhesion process. *Biomaterials* **23**, 585–596 (2002).
47. Svedhem, S. *et al.* In situ peptide-modified supported lipid bilayers for controlled cell attachment. *Langmuir* **19**, 6730–6736 (2003).
48. Thid, D. *et al.* Issues of ligand accessibility and mobility in initial cell attachment. *Langmuir* **23**, 11693–11704 (2007).
49. Bledi, Y., Domb, A. J. & Linial, M. Culturing neuronal cells on surfaces coated by a novel polyethyleneimine-based polymer. *Brain Res. Protoc.* **5**, 282–289 (2000).
50. Lakard, S. *et al.* Adhesion and proliferation of cells on new polymers modified biomaterials. *Bioelectrochemistry* **62**, 19–27 (2004).
51. Liu, B. F., Ma, J., Xu, Q. Y. & Cui, F. Z. Regulation of charged groups and laminin patterns for selective neuronal adhesion. *Colloids Surfaces B Biointerfaces* **53**, 175–178 (2006).
52. Ryu, J. R. *et al.* Synaptic compartmentalization by micropatterned masking of a surface adhesive cue in cultured neurons. *Biomaterials* **92**, 46–56 (2016).

53. Lakshminarayanaiah, N. & Murayama, K. Estimation of surface charges in some biological membranes. *J. Membr. Biol.* **23**, 279–292 (1975).
54. Pekker, M. & Shneider, M. N. *The surface charge of a cell lipid membrane*.
55. Afanasenkau, D. & Offenhäusser, A. Positively Charged Supported Lipid Bilayers as a Biomimetic Platform for Neuronal Cell Culture. *Langmuir* **28**, 13387–13394 (2012).
56. Choi, S.-E., Greben, K., Wördenweber, R. & Offenhäusser, A. Positively charged supported lipid bilayer formation on gold surfaces for neuronal cell culture. *Biointerphases* **11**, 021003 (2016).
57. Zhang, G. *et al.* Molecular Interactions between Wells−Dawson Type Polyoxometalates and Human Serum Albumin. *Biomacromolecules* **9**, 812–817 (2008).
58. Singh, P. *et al.* Unraveling the Role of Monoolein in Fluidity and Dynamical Response of a Mixed Cationic Lipid Bilayer. *Langmuir* **35**, 4682–4692 (2019).
59. Wiegand, G., Arribas-Layton, N., Heiko, H., Sackmann, E. & Wagner, P. Electrical Properties of Supported Lipid Bilayer Membranes. *J. Phys. Chem. B* **106**, 4245–4254 (2002).
60. Travaglia, A. *et al.* Electrostatically driven interaction of silica-supported lipid bilayer nanoplatforms and a nerve growth factor-mimicking peptide. *Soft Matter* **9**, 4648–4654 (2013).
61. Satriano, C. *et al.* Ferritin-supported lipid bilayers for triggering the endothelial cell response. *Colloids Surfaces B Biointerfaces* **149**, 48–55 (2017).
62. Picart, C. *Polyelectrolyte Multilayer Films: From Physico-Chemical Properties to the Control of Cellular Processes*. *Current Medicinal Chemistry* vol. 15 (2008).
63. Lee, I.-C. & Wu, Y.-C. Assembly of Polyelectrolyte Multilayer Films on Supported Lipid Bilayers To Induce Neural Stem/Progenitor Cell Differentiation into Functional Neurons. *ACS Appl. Mater. Interfaces* **6**, 14439–14450 (2014).

Chapter 3: Extracellular Vesicle Characterization

3.1. Introduction

While much attention in TEV-related studies surrounds the compositional characteristics of TEVs, physical properties may also impact the way they facilitate transfer and communication. Studies have shown that preferential targeting can be either an EV-mediated or recipient cell-mediated process[1]. One factor that plays a role in both selection processes is EV size. Evidence suggests smaller EVs lead to faster and/or preferred uptake by recipient cells and easier EV diffusion into cells via certain pathways[2,3].

Previous experiments done within the Daniel lab have revealed that TEVs begin to aggregate as soon as they are isolated leading to an increase in perceived size over time. To alleviate potential changes in cell uptake or response to EVs over multi-day studies both during these preliminary studies and during studies using the OECT model system, it is imperative to define potential aggregation patterns to determine if, at any point, fresh EVs will need to be introduced to the cell culture medium or platform. Therefore, this preliminary study will focus on a) characterizing the initial size and concentration of MV and exosome populations isolated and b) identifying whether significant aggregation will occur during later assays.

In this chapter Nanoparticle Tracking Analysis (NTA) was employed to track the movement of laser-illuminated individual TEVs under Brownian motion and calculate their diameter using statistical methods[4]. Here, size distributions and concentrations of separated MV and exosome samples were obtained and compared with established literature. Furthermore, exosome samples were analyzed over time and showed an insignificant particle aggregation rate within the experimental time parameters (72-h). As a result, it was determined that potential changes in vesicle uptake or response by cells as a result of exosome size would likely be avoided.

3.2. Materials and Methods

Cell Culture

For regular cell culture, Triple-Negative Breast Cancer cells, MDA-MB-231 (ATCC), were maintained in Dulbecco′s Modified Eagle′s Media, DMEM (Corning) supplemented with 10% FBS and 1% penicillin-streptomycin (P/S)(Corning) and used between passages 2 and 12. All cultures were split 1:5 once they reached 85% confluence. Subsequently, the medium was changed every 2 days. All cultures were kept in a humidified incubator with % CO2 at 37 °C.

For extracellular vesicle (EV) isolation, MDA-MB-231 at 85% confluency were washed with Dulbecco's phosphate-buffered saline (DPBS) (Corning) and changed to FBS-free DMEM (Corning) supplemented with 1% penicillin-streptomycin (Gibco). Following 24hrs incubation at 37°C, EVs were collected and purified.

Extracellular Vesicle Isolation

To isolate EVs, the medium was collected from the culture plates and subjected to sequential centrifugation cycles. The first spin was carried out at 4,000 rpm for 12 min, followed by an 8,000 rpm spin for 30 min. Following this centrifugation, the supernatant was filtered through a 0.22 µm Millipore Steriflip PVDF filter (Millipore) to separate MVs and exosomes. The suspected MV yield retained on top of the filter was resuspended in 1mL DPBS and stored at 4 °C for later characterization. In order to isolate the exosome population, the filtered medium was centrifuged at 32,000 rpm for 4hrs at 4°C. The supernatant was discarded, and the exosome pellet was resuspended in 1mL serum-free media and stored at 4 °C.

EV Size Distribution and Concentration

Size distribution and concentration of EVs were measured using a NanoSight NS300 (Malvern

Preanalytical). Samples were diluted at 1:10 and 1:100 for MVs and exosomes, respectively, to achieve a concentration below 10^9 particles/ml. Samples were manually inserted into the instrument using a 1mL syringe. For each sample, five videos were captured for 60 s at a camera level between 14-16. All measurements were carried out at room temperature and the chamber was cleaned 3x with DI water between each sample. Sample videos were analyzed by the NanoSight with a detection threshold set between 4-5 to obtain vesicle concentration (particles/ml) and size distribution (nm).

Exosome Aggregation Study

Size distribution and concentration of exosomes were measured using a NanoSight NS300 (Malvern Preanalytical) immediately following isolation and every 24hrs for 72hrs using the same protocol and machine settings described above for the initial EV size distribution and concentration measurements.

Data Analysis

Variance analysis was performed using a t-test with unequal variances to find significant differences between experimental conditions. Three independent replicates were performed and analyzed using Excel (Microsoft) for all experiments in this study.

3.3. Results and Discussion

Size and Concentration Distribution

Extracellular vesicles were isolated from triple-negative breast cancer cells as described in the methods section above to estimate the size distribution of the particles in the isolated MV and exosome samples. A graphical representation of the isolation protocol is shown in Figure 3.1.

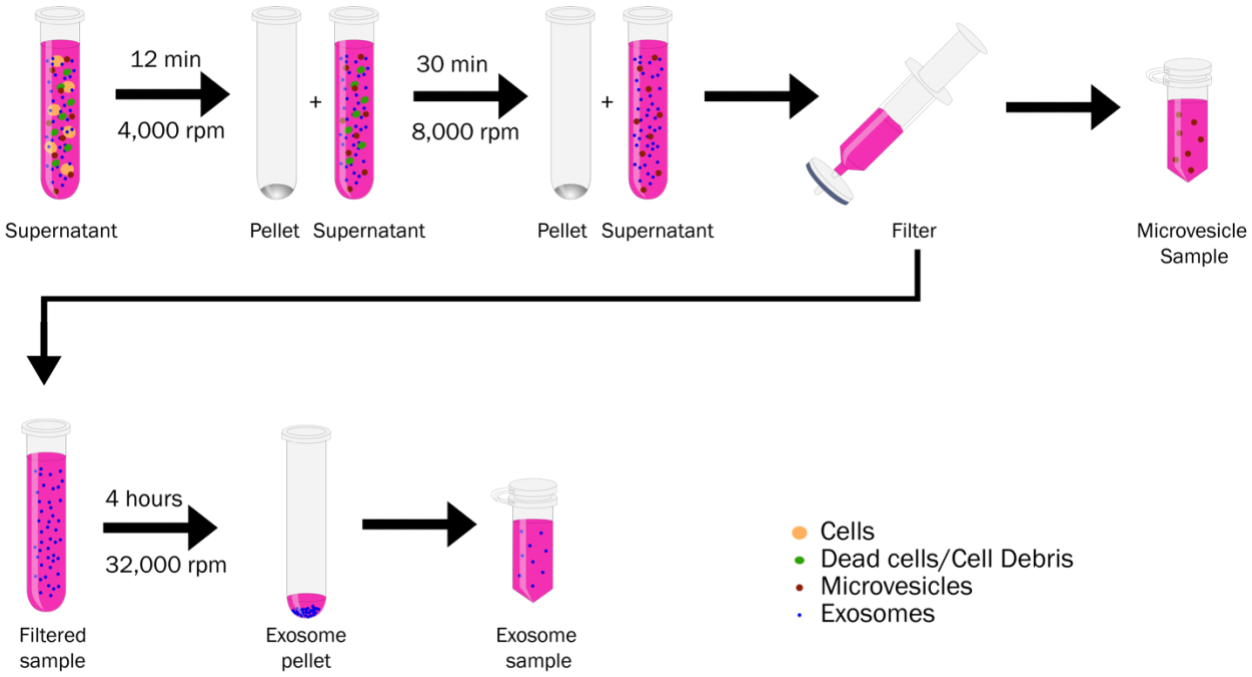

Figure 3.1. Extracellular Vesicle Isolation. Graphical Representation of the isolation protocol for MVs and exosomes through sequential centrifugation and filtration.

The average TEV size and concentration across three replicates were estimated through NTA showing an exosome concentration of $8.74 \times 10^8 \pm 3.32 \times 10^7$ particles/mL and uniform size distribution with mean particle sizes between 100 nm and 150 nm, in alignment with literature[5,6] (Fig. 3.2a). The MV samples' size distribution, on the other hand, was polydisperse with 5 population sizes (Fig. 3.2b). While the lower particle density of $6.52 \times 10^7 \pm 1.41 \times 10^6$ particles/mL and 200 nm - 450 nm size range of the particles in the 3 peaks on the right are in alignment with what literature characterizes for MVs[5,7], the size range of smaller particle population seen in the two peaks on the left suggests the presence of exosomes within the MV sample.

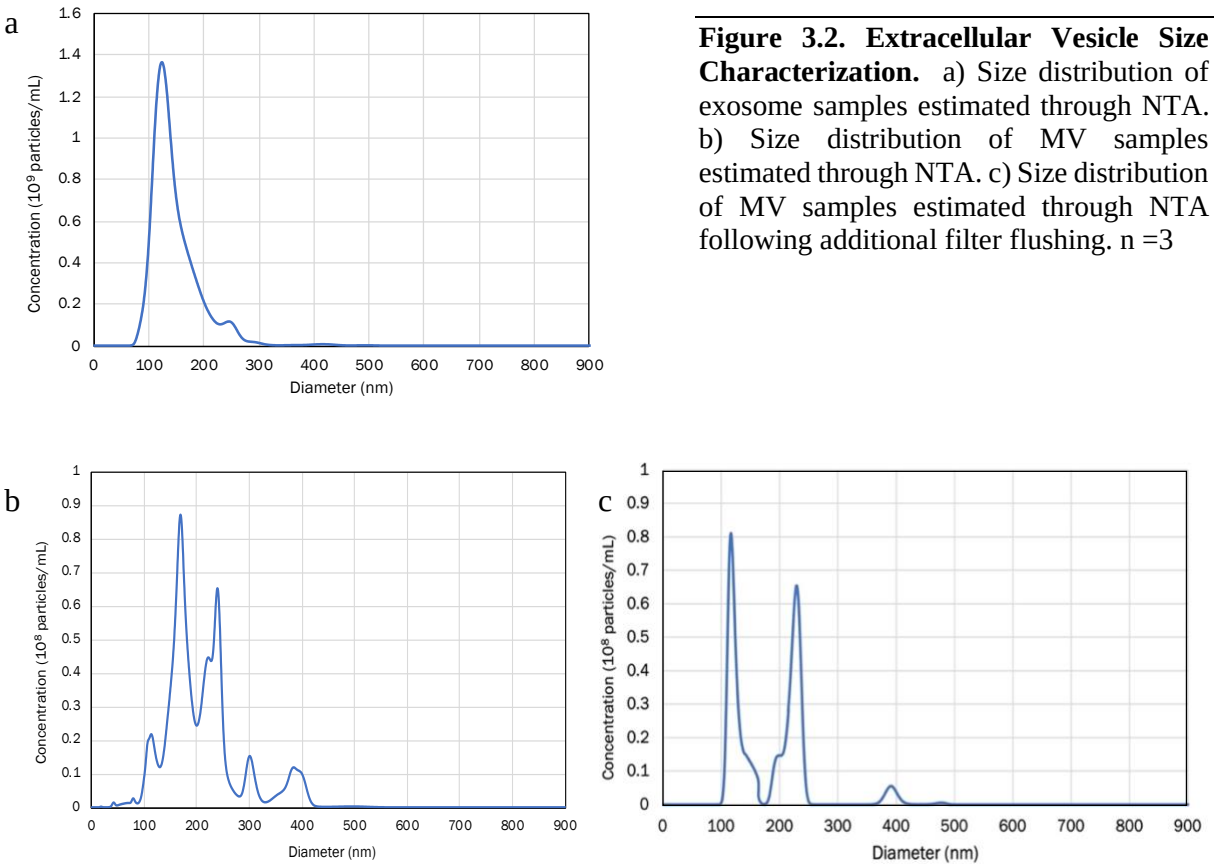

Figure 3.2. Extracellular Vesicle Size Characterization. a) Size distribution of exosome samples estimated through NTA. b) Size distribution of MV samples estimated through NTA. c) Size distribution of MV samples estimated through NTA following additional filter flushing. n =3

The low MV yield, and the likely presence of exosomes, can both potentially be explained by the plugging and retention of MVs and exosomes within the filter as a result of the high concentration of TEVs passing through or coming into contact with the filter at once. To test this theory, following the initial filtering of the supernatant to separate the exosome and MV populations, the filter was flushed 3 additional times with pure DPBS to potentially allow any remaining exosomes to pass through the filter and dislodge any MVs stuck within the filter. The bimodal distribution seen in Figure 3.2c shows that, although the presumed exosome presence was decreased, two distinct populations were still present in the sample. Furthermore, there was also no increase in MV yield revealing a need for further optimization of the MV isolation protocol. This optimization is beyond the scope of this work, however, as exosomes were solely used within the cell studies described later in this work. The observed uniform size distribution, with particles

outside of the designated exosome size range making up less than 0.5% of the particle population (Fig 3.2a), suggested the exosome samples were largely homogeneous providing sufficient evidence to proceed with future studies.

Exosome Aggregation Study

To assess the extent of vesicle aggregation within the isolated exosome samples over time, NTA was used to obtain a particle size distribution every 24hrs, for 72hrs, as described in the methods section above. Since the cell studies described later in this work were conducted over a 48hrs period, this study was conducted for 72hrs to also account for the time between exosome isolation and exposure to cells - usually 2-12 hours following isolation.

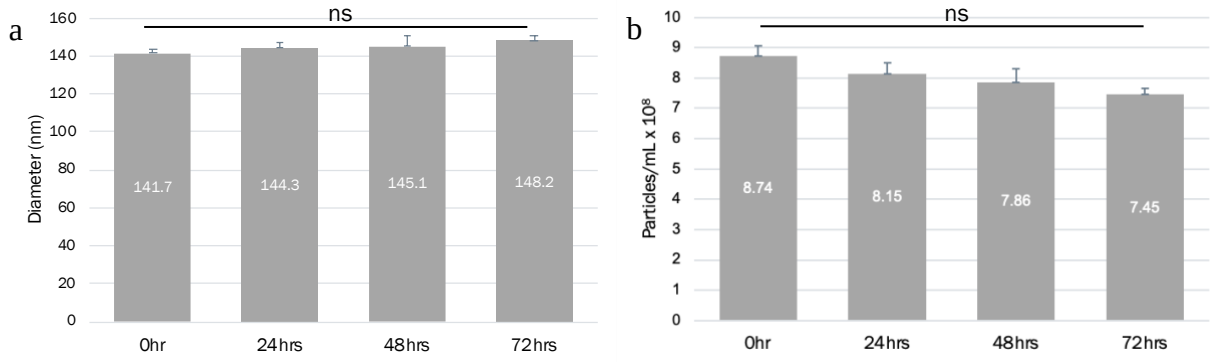

Figure 3.4. Size distributions of MDA-MB-231 exosomes over time. a) Average size of exosomes over 3 days. n = 3, mean ± SD, ns = not significant b) Average concentration of exosomes over 3 days. n = 3, mean ± SD, ns = not significant.

From Figure 3.4, aggregation can be seen by the simultaneous increase in mean particle diameter and decrease in mean concentration as would be expected of particles clumping together to physically measure as larger particles in lower concentrations. The exosome aggregation observed over the 72hrs period is minimal, however, with mean sample sizes at 72hrs measuring less than 10 nm greater than exosome sizes at initial isolation (Fig. 3.4a). With such an insignificant amount of aggregation occurring over the observed period, it was deemed safe to assume that exosome aggregation would not affect cell behavior or response during the cell studies. Therefore,

exosomes would only need to be introduced to the cells once, in the beginning, for the entirety of the experiment.

3.4. Conclusions

In this section, the size distributions and concentrations of isolated exosome and MV samples were characterized. Additionally, the size distributions of exosomes were measured over a 72hrs period and reveal an insignificant rate of aggregation during this time period. This is an important observation as it informs the best practices for exposing exosomes to cell medium and the model cell membranes of the SLB-OECT system during multi-day studies. As a result of the observations here, it is believed that exosomes will only need to be added once during the 48hrs studies performed in this work and subsequently the 48hrs studies to be performed on the SLB-OECT platform. Further testing should be performed to determine best practices for studies longer than 48hrs. The findings observed herein were extended to the 48hrs cell studies discussed in the next chapter to better understand the role of exosome uptake in angiogenesis.

3.5. References

1. French, K. C., Antonyak, M. A. & Cerione, R. A. Extracellular vesicle docking at the cellular port: Extracellular vesicle binding and uptake. *Seminars in Cell and Developmental Biology* vol. 67 48–55 (2017).
2. Caponnetto, F. *et al. Size-dependent cellular uptake of exosomes*.
3. Costa Verdera, H., Gitz-Francois, J. J., Schiffelers, R. M. & Vader, P. Cellular uptake of extracellular vesicles is mediated by clathrin-independent endocytosis and macropinocytosis. *J. Control. Release* **266**, 100–108 (2017).
4. RA, D. *et al.* Sizing and phenotyping of cellular vesicles using Nanoparticle Tracking Analysis. *Nanomedicine* **7**, 780–788 (2011).
5. Colombo, M., Raposo, G. & Théry, C. Biogenesis, Secretion, and Intercellular Interactions of Exosomes and Other Extracellular Vesicles. *Annu. Rev. Cell Dev. Biol.* **30**, 255–289 (2014).
6. Tkach, M. & Théry, C. Communication by Extracellular Vesicles: Where We Are and Where We Need to Go. *Cell* **164**, 1226–1232 (2016).
7. Han, L., Lam, E. W. F. & Sun, Y. Extracellular vesicles in the tumor microenvironment: Old stories, but new tales. *Mol. Cancer* **18**, 1–14 (2019).

Chapter 4: Cancer-Derived Exosomes in The Promotion of Angiogenesis via Vascular Endothelial Growth Factor (VEGF) Upregulation

4.1. Introduction

Rapidly growing solid tumors depend on angiogenesis, the formation of new blood vessels. Recent studies have shown that exosomes discharged by various cells can aid in this process[1,2]. As previously mentioned, TEVs supply an exchange of information between cells and can evoke a malignant chain reaction leading to enhanced tumor proliferation. In the case of angiogenesis, tumor-derived exosomes have been found to influence endothelial cells by promoting their vascular endothelial growth factor (VEGF) expression[3,4]. VEGF is a principal pro-angiogenic factor that prompts the proliferation and migration of endothelial cells and increases vascular permeability. Therefore, upregulation of VEGF contributes to tumor development and metastasis by increasing tumor-related angiogenesis[5–7].

Although many studies have investigated the ability of exosomes to regulate VEGF, great effort should be applied to recognize this process thoroughly as both recipient and secreting cell types have previously been found to induce varying effects[8]. In the present study, exosomes derived from triple-negative breast cancer cells (MDA-MB-231) were investigated for their effect on model epithelial Madin-Darby Canine Kidney (MDCKII) cells. This cell line was chosen, in part, due to initial constraints in collaborator access to human breast epithelial cell line MCF-10a and components like Cholera Toxin which is a requirement for MCF-10a cell culture medium. Nonetheless, despite being a canine cell line, MDCKII is a well-known model epithelial cell line with surplus data justifying its capability to provide physiologically relevant responses to exosomes from human cells.

Since the work described in this thesis will aid in establishing proper controls for a biomimetic electronic platform, the goal of this study was to investigate the angiogenic activity of MDCKII cells over a short-term study to elucidate any potential trends or time-dependent findings that may be referenced when repeating this study on the SLB-OECT system. Furthermore, an attempt to block exosome binding was also explored within this study since the functional effects of exosomes rely heavily on the binding, uptake, and subsequent release of cargo into recipient cells. Although the future SLB-OECT system studies are not anticipated to include drug discovery, identifying a small subset of known compounds that successfully block vesicle binding can serve as a proof of concept for the capabilities of the device as a drug testing platform. The blocking study discussed in this chapter will serve as the groundwork for one such compound, to be later corroborated by the SLB-OECT device. The results of this study show that exosome uptake contributes to the exponential upregulation of VEGF in MDCKII cells, and the treatment of exosomes with heparin can effectively prevent the upregulation of VEGF presumably due to the blockade of exosome uptake into MDCKII cells.

4.2. Methods and Materials

Cell Culture

For regular cell culture, MDCK II (Sigma) were maintained in Eagle's Minimum Essential Medium (EMEM) (Sigma) supplemented with 10% fetal bovine serum (FBS)(Gibco) and 25mM of L-Glutamine (Sigma) and used between passages 10 and 20. MDA-MB-231 (ATCC) were maintained in Dulbecco′s Modified Eagle′s Media, DMEM (Corning) supplemented with 10% FBS and 1% penicillin-streptomycin (P/S)(Corning) and used between passages 2 and 12. All cultures were split 1:5 once they reached 80-85% confluence. Subsequently, the medium was changed every 2 days. All cultures were kept in a humidified incubator with % CO2 at 37 °C.

For extracellular vesicle (EV) isolation, MDA-MB-231 at 85% confluency were washed with Dulbecco's phosphate-buffered saline (DPBS) (Corning) and changed to FBS-free DMEM (Corning) supplemented with 1% penicillin-streptomycin (Gibco). Following 24hrs incubation at 37°C, EVs were collected and purified.

For VEGF assays, MDCK II at 80% confluency were treated with 1x 0.25% trypsin at 37 °C for 7 min to detach cells. The cells were subsequently seeded at 70% confluency and cultured on three 60 mm x 15 mm cell culture dishes in the aforementioned culture medium. Once cells reached the desired 80% confluence, the culture medium was removed, and cells were washed with DPBS (Corning) and incubated with Hoechst 33342 dye (ThermoFisher) for 10min at 37 °C to stain the nuclei of the cells for visualization and counting purposes. The cells were subsequently washed 3x with DPBS and cultured in EMEM supplemented with 1% FBS and 25mM L-Glutamine for 5hrs at 37 °C prior to exposure to assay treatment conditions.

Exosome Isolation

Protocol outlined in Chapter 3.

VEGF Expression Assay

Following a 5hrs incubation period, 100µL of the supernatant was collected from each well and stored at -20 ºC. The entire exosome yield achieved from MDA-MB-231 isolation ($8.74 \times 10^8 \pm 3.32 \times 10^7$ particles/mL) was then incorporated into the media of one well, 5ng/mL TGFβ was added into the second well as a positive control, and the third well remained untreated as a negative control. Each well was then incubated at 37 °C for 48hrs. 100µL of each sample condition's media was collected at 12hrs, 24hrs, 36hrs, 39hrs, 42hrs, and 48hrs and stored at -20 ºC for ELISA. The cells were imaged at 0hrs, 24hrs, 36hrs, and 48hrs for cell counting. VEGF concentration determined through ELISA was normalized by total cell number per well.

Heparin Coating

Purified exosomes were incubated with 100 μg/ml heparin (Sigma) in serum-free media at RT for 30 min. This mixture was then added to cells[9].

Heparin Blocking Assay

Following a 5hrs incubation period, 100μL of the supernatant was collected from each well and stored at -20 ºC. Heparin-coated exosomes were then incorporated into the media of one well, exosomes without heparin incubation were added into the second well as a positive control, and the third well remained untreated as a negative control. Each well was then incubated at 37 °C for 48hrs. 100μL of each sample condition's media was collected at 12hrs, 24hrs, 36hrs, 39hrs, 42hrs, and 48hrs and stored at -20 ºC for ELISA. VEGF concentration determined through ELISA was normalized by total cell number per well.

ELISA

Enzyme-Linked Immunosorbent Assay (ELISA) was conducted according to the protocol defined by the Canine VEGF DuoSet Kit (R&D Systems) on 96-Well plates (Corning Costar). Following the addition and incubation of the TMB Substrate Solution (ThermoFisher) for 20min, the reaction was stopped by adding 0.18 M H_2SO_4, and the plates were read at a 450 nm absorbance using a microplate reader.

Fluorescence Microscopy

Fluorescent images were captured by an inverted Zeiss Axio Observer to image the fluorescently labeled nuclei of the MDCKII cells. 40-50 images were taken per well at 200x magnification.

Cell Number Calculations

Image analysis was performed using ImageJ (NIH) and Excel (Microsoft). The total number of cells per image was counted and then averaged to determine the average cells per image and standard deviation between images. Cell numbers for time points 0hrs, 24hrs, 36hrs, and 48hrs were plotted in Excel, and the best-fit line (~2-3%) equation was used to extrapolate for estimated cell number at time points not imaged. To estimate the total cell count per well, the scaling factor was determined based on the ratio between the area of the well captured within the images and the total area of the well.

Data Analysis

Variance analysis was performed using a t-test with unequal variances to find significant differences between experimental conditions. Four independent replicates were performed for this study and analyzed using Excel (Microsoft).

4.3. Results and Discussion

Exosome-Mediated Angiogenesis

The cell experiments were motivated by previous studies showing the role of exosomes in inducing angiogenesis in tumors and tumor-free tissues. In accordance with the established interaction between exosomes and certain types of epithelial cells, the introduction of MDA-MB-231 derived exosomes to the seeded MDCKII cells showed an exponential VEGF upregulation over time in comparison with the linear upregulation exhibited by cells treated with positive control TGFB, as well as with the minimal upregulation in cells that had not been treated with anything (Figure 4.1). The results with respect to time were also very promising: the impact of exosome exposure was not observed until approximately 36hrs after the addition of the exosomes to the cell culture medium. This finding contrasts the consistent upregulation observed of TGFB treated cells which was to be expected as TGFB is known to increase VEGF secretion and promote

angiogenic activity[10]. Interestingly, though, even with a delayed response, the VEGF expression of exosome-treated cells surpassed that of TGFB treated cells within 6hrs. Moreover, the VEGF expression from the exosome-treated cells at 48hrs was observed to be over 2x greater than TGFB treated cells at the same time point and almost 4x greater than the initial expression (0hrs) of the same treatment condition.

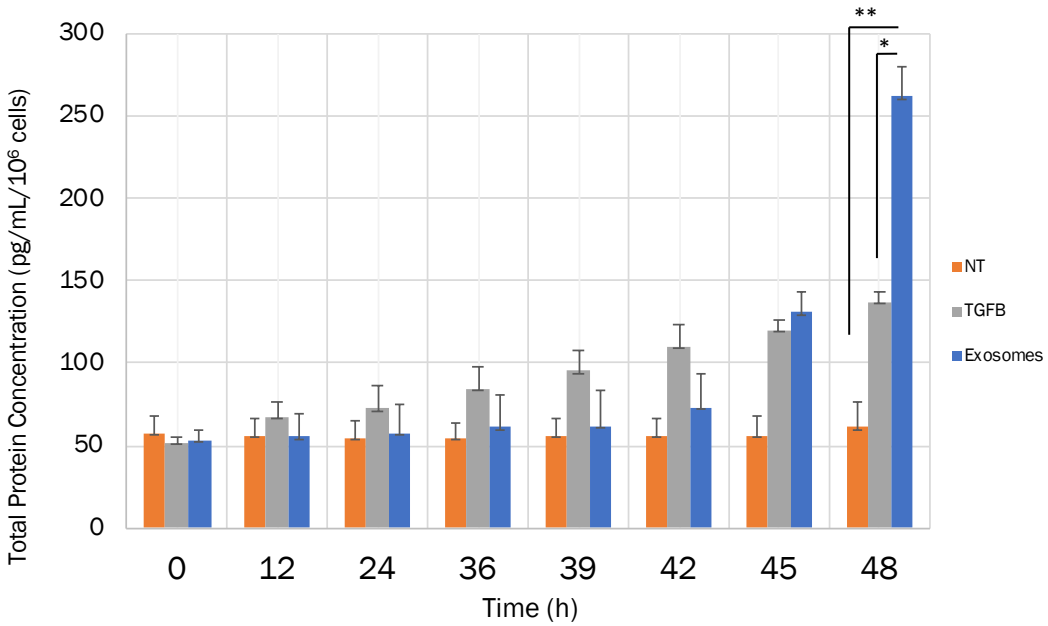

Figure 4.1. VEGF expression over time. Total VEGF expressed over 48 hours by MDCKII cells treated with breast cancer-derived exosomes, TGFB, or no treatment (NT). n = 4, mean ± SD, * = $p \leq 0.05$, ** = $p \leq 0.01$

These results support the hypothesis that exosomes from triple-negative breast cancer cells possess the potential to upregulate VEGF signaling in epithelial cells. Although the mechanisms underlying this data remains unclear, the notable exponential and time-dependent trends are seen here serve as clear reference data for future studies aiming to further probe the exosome uptake and cargo release processes.

Blocking Exosome Uptake with Heparin

To determine if exosome uptake could be inhibited, exosomes derived from MDA-MB-231 cells were pretreated with heparin and introduced to the MDCKII cell culture medium as described in the methods section. The heparin-treated exosome condition showed effective blocking of exosome-mediated VEGF upregulation. This can be seen in Figure 4.2 as the heparin treated condition mimics the same minimal upregulation as was observed of the untreated condition.

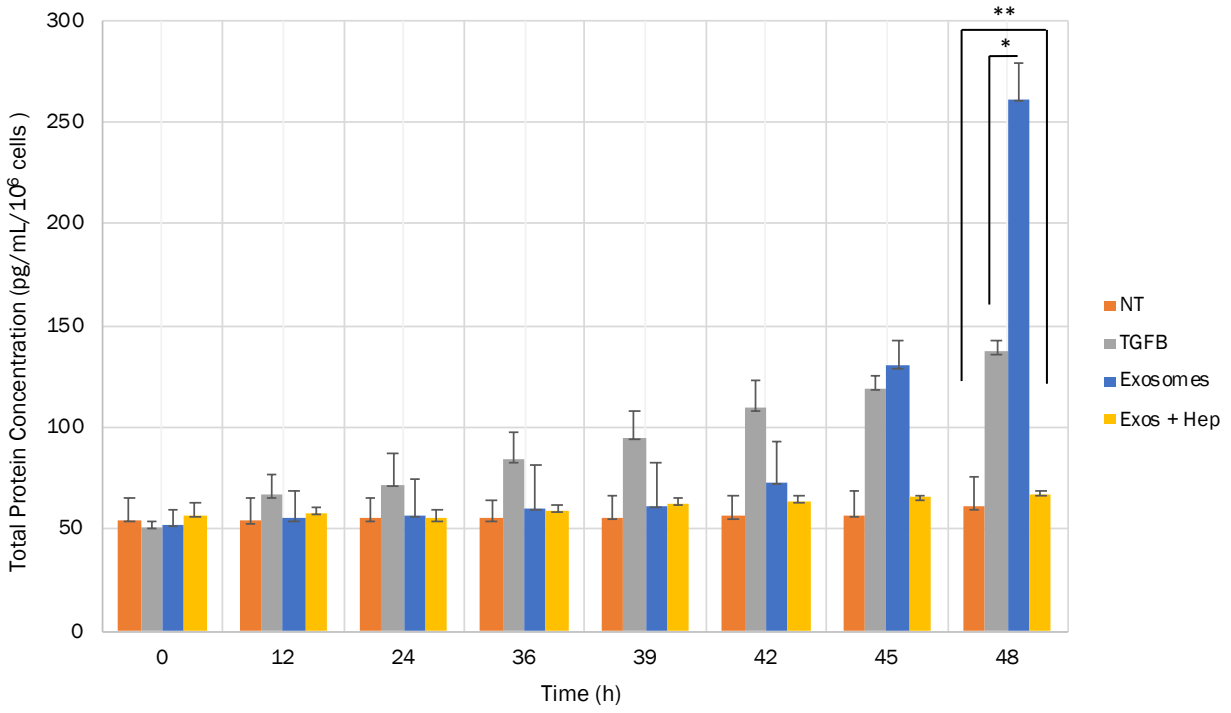

Figure 4.2. VEGF expression over time with heparin. Total VEGF expressed over 48 hours by MDCKII cells treated with heparin-coated exosomes, breast cancer-derived exosomes, TGFB, or no treatment (NT). n = 3, mean ± SD, * = $p \leq 0.05$, ** = $p \leq 0.01$

Since more than one route can be taken to internalize exosomes, the heparin's interference with exosome uptake may have occurred via more than one process. The use of heparin here referenced several studies which showed heparin may act as a decoy for exosome receptors such as heparin sulphate proteoglycans, effectively preventing them from binding with cells[9,11,12].

Furthermore, since in this study, the excess heparin not bound to exosome receptors was not removed from the exosome sample, it is possible that heparin also bound to MDCKII surface receptors acting as a secondary blockage from exosomal binding and uptake. Although these results are preliminary and these hypotheses were not investigated, future studies may unveil the mechanisms involved in the regulating effects of heparin and provide further insight into how it can be used to limit the effects of cancer-derived exosomes.

4.4. Conclusions

In summary, exosomes derived from MDA-MB-231 cells were found to possess a higher capacity to enhance angiogenesis *in vitro* via VEGF signaling when compared to control conditions. Markedly, VEGF expression began to upregulate exponentially at 36hrs, suggesting this to be the potential time needed to effectively complete the binding, uptake, release, and response processes. The ability to block exosome uptake was also explored. Treating exosomes with heparin was found to effectively prevent VEGF upregulation suggesting exosome blocking was successful. Further study using the SLB-OECT platform is anticipated to be able to test these hypotheses and elucidate the mechanisms involved in each of these processes.

4.5. References

1. Ghorbanian, M., Babashah, S. & Ataei, F. The effects of ovarian cancer cell-derived exosomes on vascular endothelial growth factor expression in endothelial cells. *EXCLI J.* **18**, 899–907 (2019).
2. Cho, J. A., Park, H., Lim, E. H. & Lee, K. W. Exosomes from breast cancer cells can convert adipose tissue-derived mesenchymal stem cells into myofibroblast-like cells. *Int. J. Oncol.* **40**, 130–138 (2012).
3. Webber, J., Steadman, R., Mason, M. D., Tabi, Z. & Clayton, A. Cancer exosomes trigger fibroblast to myofibroblast differentiation. *Cancer Res.* **70**, 9621–9630 (2010).
4. Chowdhury, R. *et al.* Cancer exosomes trigger mesenchymal stem cell differentiation into pro-angiogenic and pro-invasive myofibroblasts. *Oncotarget* **6**, 715–731 (2015).
5. Lee, J. K. *et al.* Exosomes derived from mesenchymal stem cells suppress angiogenesis by down-regulating VEGF expression in breast cancer cells. *PLoS One* **8**, 84256 (2013).
6. Shahi, P. K. & Pineda, I. F. Tumoral angiogenesis: Review of the literature. *Cancer Investigation* vol. 26 104–108 (2008).
7. Welti, J., Loges, S., Dimmeler, S. & Carmeliet, P. Recent molecular discoveries in angiogenesis and antiangiogenic therapies in cancer. *Journal of Clinical Investigation* vol. 123 3190–3200 (2013).
8. Ludwig, N., Yerneni, S. S., Razzo, B. M. & Whiteside, T. L. Exosomes from HNSCC Promote Angiogenesis through Reprogramming of Endothelial Cells. *Mol Cancer Res* **16**, (2018).
9. Atai, N. A. *et al.* Heparin blocks transfer of extracellular vesicles between donor and recipient cells. *J. Neurooncol.* **115**, 343–351 (2013).
10. Ferrara, N. & Davis-Smyth, T. The Biology of Vascular Endothelial Growth Factor. *Endocr. Rev.* **18**, 4–25 (1997).
11. Christianson, H., Svensson, KJvan Kuppevelt, T., Li, J. & Belting, M. Cancer cell exosomes depend on cell-surface heparan sulfate proteoglycans for their internalization and functional activity. *Proc. Natl. Acad. Sci. U. S. A.* **110**, 17380–17385 (2013).
12. Maguire, C. A. *et al.* Microvesicle-associated AAV Vector as a Novel Gene Delivery System. *Mol. Ther.* **20**, 960 (2012).

Chapter 5: Summary and Future Work

5.1. Summary of Results

The studies I conducted in this thesis were not only able to provide relevant size and concentration characterizations for TEV derived from triple-negative breast cancer cells but also demonstrate the ability of TEVs, specifically exosomes, to regulate the angiogenic behavior of model epithelial cells. The isolation protocol and use of NTA revealed the need for additional measures to purify isolated MV populations as I observed two distinct populations suggesting a notable exosome presence contaminating the MV samples. The isolated exosome samples, on the other hand, appeared largely pure with a single, uniform size distribution of particles. Using NTA, I also monitored the aggregation of exosomes finding sufficient evidence that while aggregation does occur within the exosome samples, the aggregation rate was minimal for at least 72 hours following isolation. As a result, cells were only infected with exosomes once, at the beginning of the 48hrs experiments conducted, since the slight increase in size eliminated the need to add another batch of freshly isolated exosomes at any point during the experimental period.

In the cell experiments, cells were treated with exosomes and observed for 48hrs to assess the ability of exosomes to induce pro-angiogenic behavior in epithelial cells via VEGF expression. When stimulated with exosomes, I observed an exponential upregulation of VEGF about 36 hours following exosome exposure indicating an increase in angiogenic activity within the epithelial MDCKII cells. This trend was notably different than the linear upregulation seen in the positive control, TGFB treated sample, as well as the near-constant VEGF expression seen in the negative control with no treatments. To determine whether the effects of exosome infection could be circumvented, I attempted to block the initial binding and uptake of exosomes altogether by using heparin to potentially block the receptors needed for exosomes to bind with cells. Here, I

demonstrated the reversal of exosome-mediated VEGF upregulation as cells treated with heparin-coated exosomes showed behavior consistent with cells that had no treatment suggesting exosomes were unsuccessful in either binding or being taken up into the MDCKII cells. While I was able to show that exosomes can induce angiogenesis with VEGF signaling and that heparin can prevent this, time was a prominent limitation preventing me from being able to further explore the mechanisms involved in these processes. However, the SLB-OECT platform to be developed will allow for an in-depth compositional and mechanistic analysis of the mechanisms promoting the outcomes observed in these studies.

5.2. Future Work

As mentioned in Ch. 1, many milestones are necessary to successfully develop and optimize the SLB-OECT platform described in this thesis. While additional cell studies and TEV characterizations were simultaneously being performed by collaborators and other members of the Daniel lab, milestones 4 and 5 will serve as the direct next steps following the experimental work performed in this thesis. Briefly, these milestones would be to document and characterize the electrical readouts of the interplay between exosomes and epithelial cells on OECTs during the exosome infection and heparin blocking processes. This data combined with the trends and time data I acquired here will educate device users on what the electrical readouts represent in live TEV-cell interactions allowing for design improvements and implementations to recapitulate this study with TEVs on the model SLB-OECT platform.

Additional routes for future studies, specifically cell studies, is to perform these experiments with MVs once the purification process is improved. With the understanding that MVs and exosomes may carry different cargo or undergo separate uptake processes, it would be beneficial to determine if MVs will evoke a different cell response. Additionally, it may be useful

to attempt additional compounds for blocking TEV uptake. As mentioned previously, there are multiple routes in which a cell can internalize TEVs, so there are most certainly multiple compounds that may be capable of interfering with TEV uptake. Exploring a few of these compounds in cell studies and ultimately the SLB-OECT platform will assist in enhancing the capabilities of the SLB-OECT system as a potential drug testing platform.